

See discussions, stats, and author profiles for this publication at: <https://www.researchgate.net/publication/234087743>

Two-dimensional electronic spectroscopy of CdSe nanoparticles at very low pulse power

ARTICLE in THE JOURNAL OF CHEMICAL PHYSICS · JANUARY 2013

Impact Factor: 2.95 · DOI: 10.1063/1.4772465 · Source: PubMed

CITATIONS

21

READS

38

6 AUTHORS, INCLUDING:



Graham B Griffin

DePaul University

21 PUBLICATIONS 314 CITATIONS

SEE PROFILE



Sandrine Ithurria

École Supérieure de Physique et de Chimie In...

34 PUBLICATIONS 743 CITATIONS

SEE PROFILE



Dmitriy Dolzhenkov

University of Chicago

19 PUBLICATIONS 207 CITATIONS

SEE PROFILE



Dmitri V Talpin

University of Chicago

160 PUBLICATIONS 16,259 CITATIONS

SEE PROFILE

Two-dimensional electronic spectroscopy of CdSe nanoparticles at very low pulse power

Graham B. Griffin, Sandrine Ithurria, Dmitriy S. Dolzhnikov, Alexander Linkin, Dmitri V. Talapin et al.

Citation: *J. Chem. Phys.* **138**, 014705 (2013); doi: 10.1063/1.4772465

View online: <http://dx.doi.org/10.1063/1.4772465>

View Table of Contents: <http://jcp.aip.org/resource/1/JCPSA6/v138/i1>

Published by the [AIP Publishing LLC](#).

Additional information on J. Chem. Phys.

Journal Homepage: <http://jcp.aip.org/>


Journal Information: http://jcp.aip.org/about/about_the_journal

Top downloads: http://jcp.aip.org/features/most_downloaded

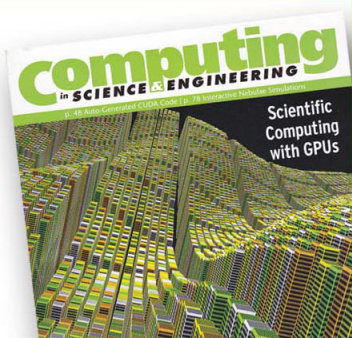
Information for Authors: <http://jcp.aip.org/authors>

ADVERTISEMENT

**SHARPEN YOUR
COMPUTATIONAL
SKILLS.**



Subscribe for
\$49 | year



computing
in **SCIENCE & ENGINEERING**

Scientific
Computing
with GPUs

Two-dimensional electronic spectroscopy of CdSe nanoparticles at very low pulse power

Graham B. Griffin,¹ Sandrine Ithurria,¹ Dmitriy S. Dolzhenkov,¹ Alexander Linkin,¹ Dmitri V. Talapin,^{1,2} and Gregory S. Engel^{1,a)}

¹*The James Franck Institute and Department of Chemistry, The University of Chicago, Chicago, Illinois 60637, USA*

²*Center for Nanoscale Materials, Argonne National Lab, Argonne, Illinois 60439, USA*

(Received 24 September 2012; accepted 3 December 2012; published online 4 January 2013)

Nanoparticles have been proposed as a promising material for creating devices that harvest, transport, and manipulate energy and electrons. Ultrafast charge carrier dynamics represent a critical design aspect and are dependent on both size and shape of the nanoparticle. Spectroscopic investigation of the electronic structure and dynamics of these systems is complicated by sample inhomogeneity, which broadens peaks and leads to ambiguity in interpretation of both spectra and dynamics. Here, we use two-dimensional electronic spectroscopy to remove inhomogeneous broadening and to clarify interpretation of measured dynamics. We specifically investigate the effect of nanoparticle shape on the electronic structure and ultrafast electronic dynamics in the band-edge exciton states of CdSe quantum dots, nanorods, and nanoplatelets. Particle size was chosen to enable straightforward comparisons of the effects of particle shape on the spectra and dynamics without retuning the laser source. The spectra were measured with low pulse powers (generally <1 nJ/pulse), using short pulses (~ 12 fs) to minimize interference from solvent contributions to the spectra, ambiguities in the dynamics due to pulse-overlap effects, and contributions to the dynamics from multi-exciton effects. The lowest two exciton states are clearly resolved in spectra of quantum dots but unresolved for nanorods and nanoplates, in agreement with previous spectroscopic and theoretical results. In all nanoparticles, ultrafast dynamics measurements show strong evidence of electronic relaxation into the lowest energy exciton state within ~ 30 fs, a timescale not observable in previous dynamics measurements of similar systems. These dynamics are unambiguously assigned to hole relaxation, as the higher lying electronic excited states are not energetically accessible in these experiments. Clear evidence of coherent superpositions of the lowest two exciton states were not seen in any of the particles studied, in contrast to recent results from work on quantum dots. © 2013 American Institute of Physics. [<http://dx.doi.org/10.1063/1.4772465>]

INTRODUCTION

Semiconductor nanocrystals have been of great interest in recent years due to a number of potential applications including light-emitting diodes, photovoltaics, lasers, detectors, biolabels, and quantum information.^{1–6} CdSe quantum dots (QDs) and nanorods (NRs) present a popular experimental target due to their tractable synthesis and spectroscopically convenient size-tunable electronic transitions. The size dependent properties of semiconductor nanocrystals were first discovered decades ago,^{7,8} and since that time CdSe QDs and NRs have been characterized using various spectroscopic techniques including linear absorption,^{4,9–11} photoluminescence,^{4,12–15} and fluorescence line narrowing.¹⁶ More recently four-wave mixing techniques, such as transient absorption,^{1,11,17–25} transient grating,^{26,27} photon echo peak shift,^{28,29} and two-dimensional electronic spectroscopies,^{30,31} have been employed to measure both electronic structure and relaxation dynamics in CdSe nanocrystals.

Investigation of the electronic structure of QDs using absorption or hole-burning spectroscopies reveals dis-

crete transitions to excitonic states consisting of two interacting charge carriers, the valence band hole and conduction band electron. The energies of these transitions depend strongly on nanocrystal size, with stronger confinement of the charge carriers leading to higher energy transitions. These transitions can be assigned using a simple “particle in a sphere” model,³² but the states cannot be fully resolved spectroscopically due to inhomogeneous broadening caused by the finite size distribution of nanocrystal samples, as well as inhomogeneity in shape and surface defects.⁶ Coupling state-of-the-art size selection techniques with photon echo spectroscopy removes much of this inhomogeneity, allowing clearer elucidation of nanocrystal properties such as excitonic fine structure,^{30,33} spin relaxation,²⁶ multi-exciton effects,³⁴ and electron-phonon coupling.³⁵ This work provides data for comparison with theoretical results modeling spectra and dynamics in CdSe nanocrystals, in which the size of the nanocrystal under consideration can be uniquely specified. “Particle in a sphere” models explain the size dependence of nanocrystal absorption and luminescence, but fail to describe even some of the more simple aspects of QD electronic properties, such as the fluorescence Stokes shift. More complex methods such as the multiband effective mass

^{a)} Author to whom correspondence should be addressed. Electronic mail: gsengel@uchicago.edu.

approximation approach,^{5,12} semi-empirical pseudopotential method,^{36–40} and *ab initio* calculations^{3,41–43} correct the failings of “particle in a sphere” models but often produce fundamentally different results from one another. The optimal method for calculations of the spectral and dynamical properties of nanocrystals remains a matter of much debate.³

The ultrafast dynamics of charge carrier relaxation prove critical to many possible applications, especially in photovoltaics where Auger effects in multi-carrier relaxation have been extensively characterized in QDs.^{21,44–46} Relaxation dynamics are measured by assigning changes in the observed intensity of spectroscopic features over time to population dynamics among the excitonic states of the nanocrystal, often tracking state-filling following excitation to a high-lying excited state. These works demonstrate that nonradiative relaxation in nanocrystals containing multiple excitons can proceed by an Auger mechanism whereby the energy resulting from electron-hole recombination of one exciton re-excites a different exciton into a higher lying excited state. This mechanism significantly reduces the number of phonons that must be created to conserve energy upon exciton recombination, accelerating nonradiative relaxation by several orders of magnitude.⁴⁴ This effect is strongly dependent upon Coulomb interaction between the electron and hole, and thus relaxation rates are strongly dependent on particle volume. In QDs containing only a single hot exciton, nonradiative relaxation must proceed by transfer of electronic energy into phonons. Careful choice of the surface capping groups has also allowed investigation of the effects of surface trapping on intraband relaxation dynamics in both electron and hole states.^{19,21,46,47}

Experimental^{11,45,48} and theoretical^{42,49,50} determination of the shape dependence of transition energies and exciton relaxation dynamics have been explored using NRs. The electronic structure of NRs is substantially more complex than the QD, depending strongly on both particle size parameters (radius and rod length). The excitonic transitions are less well resolved and evolve towards the continuous band structure of a quantum wire with increasing aspect ratio (length/diameter), complicating interpretation of both spectra and dynamics, and thus ultrafast relaxation dynamics of NRs are less thoroughly characterized than those in QDs. Transient bleaching spectra show that high-lying excited states decay more quickly in NRs than in QDs, with decay becoming longer as excited state energy decreases. The dependence of relaxation dynamics on particle shape was assigned to better energy matching with phonon modes in the rods, due to splitting of degenerate states caused by the reduction in symmetry.¹¹ As the crystal shape evolves from spherical towards a more elongated structure, the degenerate states of spherical particles split into multiple closely spaced bands, allowing better energy matching of electronic relaxation with the available phonon spectrum. Auger relaxation of charge carriers in NRs has also been investigated,⁴⁵ with similar results to the analogous studies on QDs.

Recently, a new form of CdSe nanocrystal has been synthesized, the nanoplatelet (NPL).⁵¹ These particles are planar, extending in two dimensions with the third dimension controllably set to 4–7 monolayers. Excitons in these nanocrystals are thus confined in only one dimension. These NPL nanocrystals

have been characterized using high resolution transmission electron microscopy (TEM) and powder X-ray diffraction to determine size and crystal structure, to examine the formation mechanism, and to characterize their optical properties. Linear spectra of NPLs show a well-resolved band structure, with the two lowest features assigned to the heavy-hole and light-hole excitonic transitions.^{52,53} The linear spectra show substantially less inhomogeneity than the spectra of similar QD or NR nanocrystals due to the precisely controlled confinement in the third dimension, but the resonance energies are not as smoothly tunable as the other nanocrystals, being confined instead to a discrete energy for each number of monolayers. Optical transition energies of the NPLs were modeled well by a multiband effective-mass approximation originally developed by Pidgeon and Brown to describe Landau levels of InSb.⁵²

In the work presented here, we employ two-dimensional electronic spectroscopy to measure relaxation dynamics in the lowest-lying excited states of CdSe QDs, NRs, and NPLs. We investigate the effects of nanocrystal shape on electronic structure and relaxation dynamics, leveraging the ability of photon echo spectroscopy to remove inhomogeneous broadening. This improved spectral resolution allows us to clearly identify the excitonic states observed. We simultaneously measure relaxation dynamics with a time resolution of approximately 15 fs, faster than many previous measurements. The NPL spectra represent the first dynamic and nonlinear spectroscopic measurements made on these novel nanostructures. In addition, 2DES allows us to look for signatures of coherent superpositions of electronic states.

EXPERIMENT

Nanoparticle preparation

Chemicals

Trioctylphosphine oxide (TOPO, 99%, Aldrich), trioctylphosphine (TOP, 97%, Strem), Selenium (powder, 99.99%, Aldrich), tributylphosphine (TBP, 97%, Aldrich), tetradecylphosphonic acid (TDPA, 99%, Polycarbon), cadmium oxide (99.995%, Aldrich), cadmium acetate hydrate (Cd(Ac)₂, Aldrich), oleic acid (OA, 90%, Aldrich), and 1-octadecene (ODE, 90%, Aldrich).⁵⁴

Wurtzite CdSe quantum dot preparation⁵⁵

In a three neck flask, 120 mg of CdO, 560 mg ODP, and 6 g TOPO were degassed for 1 h at 150 °C. The three neck flask was then put under nitrogen flow and heated to 370 °C. Then 3 g TOP were injected, the three neck flask was reheated back to 370 °C, and 0.888 g TOPSe 1.7 M were injected. The reaction was stopped after 3 min. The NCs were then precipitated with ethanol three times and dispersed in toluene.

Wurtzite CdSe nanorod preparation⁵⁶

In a three neck flask, 0.200 g CdO, 0.895 g TDPA, and 2.9 g TOPO were degassed at 150 °C for 1 h. The mixture

was heated under flowing nitrogen at 300 °C in order to get a clear solution of Cd(TDPA)₂. Then the mixture was degassed at 150 °C for 2 h and finally the precursors were aged for 24 h under nitrogen flow.

Finally, the mixture was heated to 320 °C. A solution of 0.260 g TBPSe (25% selenium by mass) was mixed with 1.5 g TOP and 0.3 g toluene and quickly injected. The temperature of the reaction dropped down to 250 °C and was kept at this temperature for 7 min. The nanocrystals were precipitated three times with toluene and methanol and dispersed in toluene.

Wurtzite CdSe nanoplatelet preparation⁵²

In a three neck flask, 170 mg Cd(Myristate)₂ and 14 ml ODE were degassed for 30 min at room temperature. Then, under nitrogen flow, the flask was heated at 240 °C and 1 ml selenium powder dispersed in ODE by sonication was injected (Selenium in ODE at 0.15 M). After 20 s, 60 mg Cd(Ac)₂ were introduced. After 5 min at 240 °C, the mixture was cooled and 2 ml of oleic acid and 15 ml of hexane were added. The mixture was then centrifuged and the precipitate containing the nanoplatelets was washed three times with ethanol. The nanoplatelets were then suspended in a nonpolar solvent such as hexane or toluene.

Two-dimensional electronic spectroscopy

A Ti:Sapphire femtosecond laser system (Coherent Mira oscillator, Coherent Legend Elite regenerative amplifier) is used to produce a 5 kHz train of 550 mJ, 100 fs pulses with ~12 nm bandwidth centered near 800 nm. These pulses are used to pump a NOPA (Light Conversion TOPAS White), creating 20 μJ pulses with ~70 nm bandwidth centered around 550 nm, also at 5 kHz. Pulses emerge from the NOPA with substantial temporal chirp, and are compressed using a prism compressor and a pulse shaper (femtoJock, Biophotonic Solutions) in sequence. This compression scheme is configured to precompensate for all subsequent glass to ensure the pulses are optimally compressed at the sample position. After compression, pulses are 10–12 fs full width at half maximum, and proper compression is verified daily by transient-grating frequency resolved optical gating (TG-FROG), as shown in the supplementary material.⁵⁴

Two-dimensional electronic spectroscopy was performed on a passively phase stabilized spectrometer detailed in Refs. 57–59, and only a brief summary is presented here. The pulse is split using a 50:50 beamsplitter; then, a retroreflector mounted on a translation stage is used to create a time delay between the two pulses. During measurement this time delay, known as the waiting time and denoted *T*, occurs between the second and third pulses that interact with the sample. The two beams are focused onto a diffractive optic, and a mask is used to select the four outgoing first order diffraction spots, creating two pairs of phase-locked beams arranged in a boxcar geometry. A spherical mirror focuses all four beams into the sample with a spot diameter of ~50 μm.

One of the four beams is attenuated by a factor of 1000 and used as a local oscillator (LO) for heterodyne detection of the signal field. The other 3 beams are passed through pairs of 1° glass wedges, which are used for fine control of the time delays between the pulses. Two of the wedge pairs are mounted on translation stages, allowing scanning of the delay between the first two pulses to interact with sample, known as the coherence time, *τ*, over a range of ±600 fs. Phase matching considerations dictate that in the boxcar geometry the signal field created by the interaction of three of the pulses with the sample be emitted in the outgoing direction of the fourth pulse, ensuring overlap of the LO and the signal field. The signal field is collected and collimated with an off-axis parabolic mirror and directed into a 0.3 m spectrometer (Andor Shamrock), and the interferogram between the LO and the signal field is detected using a CCD camera (Andor Newton).

When measuring a two-dimensional electronic spectrum (2DES), interferograms are measured as coherence time is scanned at regular intervals using the glass wedge pairs, keeping waiting time constant. Positive coherence times (pulse 1 arriving before pulse 2) result in a photon echo signal being emitted in the phase-matched direction, and a 2DES resulting from this measurement is called a “rephasing spectrum.” Negative coherence times (pulse 2 arriving first) result in a free induction decay signal being emitted in the phase-matched direction, and a 2DES created in this way is called a “nonrephasing spectrum.” 2DES generated from scans over all coherence times are called “combined spectra.” Processing the sequence of interferograms into a two-dimensional spectrum is described in Ref. 57, and involves scatter subtraction and Fourier transform over the coherence time delay. After processing at full available resolution, data were binned into ~25 cm⁻¹ pixels in order to make processing and analysis more computationally tractable. More information on data binning can be found in the supplementary material.⁵⁴ To measure dynamical information, 2DES are measured at a sequence of waiting times covering the time domain of interest. All spectra in this work are presented as “absolute value” spectra. Due to technical limitations, phasing procedures used to separate real and imaginary parts of the signal were not carried out. As a consequence, line shapes are less well resolved than they would be in corresponding plots of the purely absorptive part of phased spectra.

Typical pulse power at the sample during experiments was 0.5–2.0 nJ/pulse in each of the three beams, and the 10 Hz power stability was measured before and after each experiment at ~1% (*σ*/mean) over the time required to measure a 2DES (3 min). The pulse power was minimized to reduce contamination of the observed spectra by nonresonant solvent response during pulse overlap. Working in this power regime also helps to eliminate multi-exciton effects, because we expect substantially fewer than one excitation per nanoparticle.⁶⁰ Experiments at higher powers were performed and are mentioned briefly below. Detailed consideration of solvent response and its role in high pulse power experiments is included in the supplementary material.⁵⁴ The sample was kept continuously recirculating through the sample cell (200 μm optical path) using a peristaltic pump. The

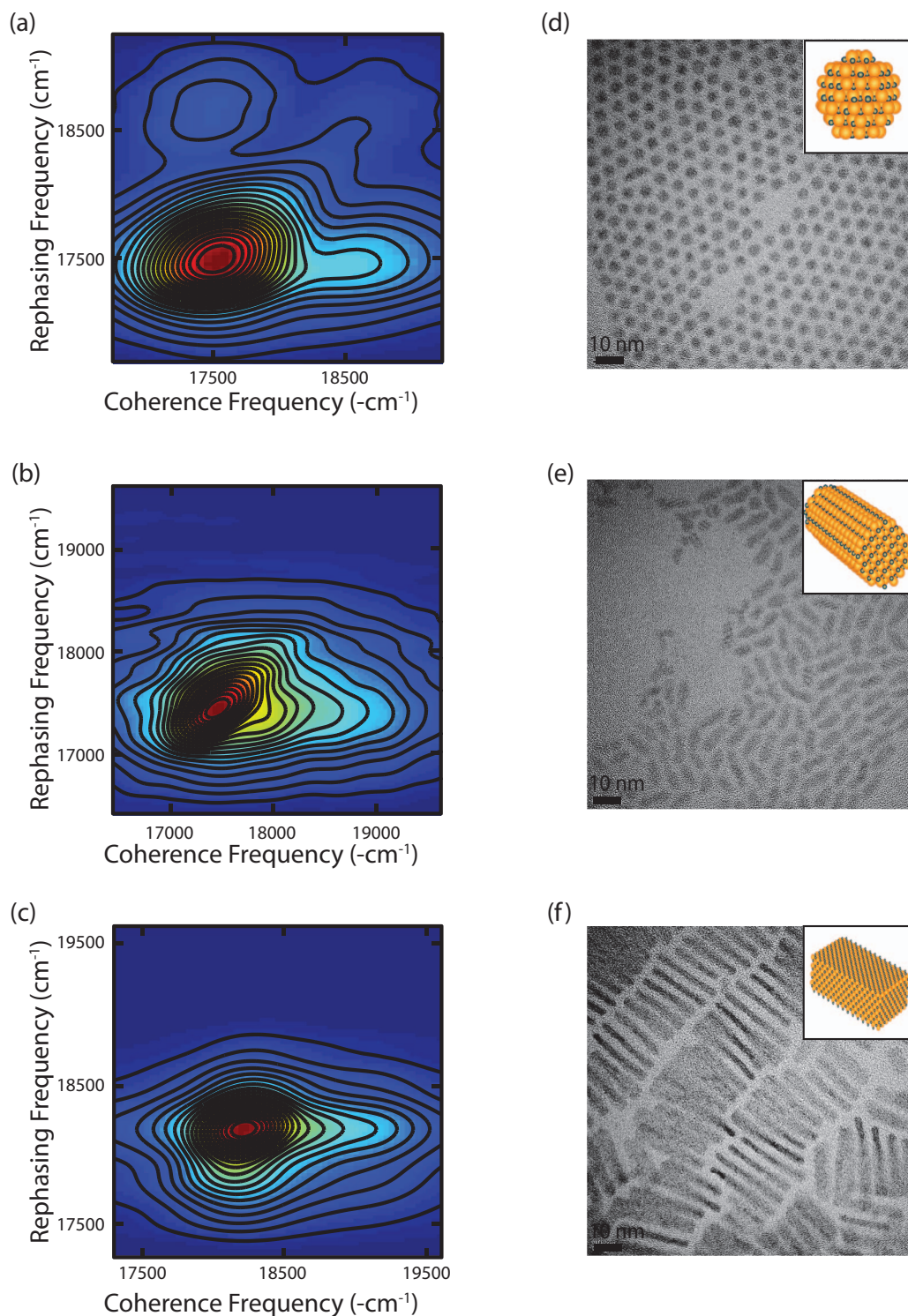


FIG. 1. Rephasing 2DES of CdSe (a) QDs at $T = 75$ fs and 0.5 nJ/pulse, (b) NRs at $T = 100$ fs and 1 nJ/pulse, and (c) NPLs at $T = 100$ fs and 0.6 nJ/pulse. These spectra are typical of all rephasing 2DES measured at waiting times longer than ~ 40 fs. TEM images of CdSe (d) QDs, (e) NRs, and (f) NPLs. The black bars on the TEM images represent a length scale of 10 nm. Illustrations of nanoparticle structure are shown in the inset of (d)–(f).

total sample volume used was typically ~ 4 ml, with ~ 2 ml in the tubes and sample cell at any given time and a flow rate sufficient to insure that each set of laser pulses hits fresh sample. Measurements of solvent response (toluene for QDs and NRs, hexanes for NPLs) were taken after every experiment at identical conditions, by flowing pure solvent into the sample cell.

RESULTS

Two-dimensional electronic spectra

Typical rephasing 2DES of QDs, NRs, and NPLs at waiting times longer than $T \approx 40$ fs are presented in Fig. 1, along with TEM images of the samples. We choose to show rephasing spectra only to simplify interpretation. Similar

spectral features and dynamics are observed in nonrephasing and combined spectra, and comparison of combined, rephasing, and nonrephasing 2DES is presented in the supplementary material.⁵⁴ To first order, interpretation of 2DES can be considered using an “energy-in/energy-out” picture in order to rationalize the position of spectral features and account for simple exponential dynamics. In this picture, we assume that the first two pulses interact with the sample at the same energy, and likewise interaction with the third pulse and emitted signal field also have the same energy as one another. The position of a feature along the coherence frequency (ω_{coh}) axis represents the energy that goes into the system upon excitation, and the position along the rephasing frequency (ω_{reph}) axis represents the energy that comes out of the system as a signal field some time, T , later. Within the simple “energy-in/energy-out” model, features appearing along the diagonal correspond to linear absorption features. Features appearing below the diagonal can be caused by relaxation from the initially excited state to a lower lying state, and should show exponentially increasing intensity with increasing waiting time. More detailed analysis of 2DES in terms of Feynman pathways enables interpretation of oscillating signals, features above and below the diagonal caused by coupling between the states, and above diagonal features usually assigned to excited state absorption. It will not be necessary to use this more detailed picture to interpret the spectra and dynamics observed in these experiments, but an example of analysis in terms of Feynman pathways is presented in the supplementary material for the interested reader.⁵⁴ In the analysis presented below, the location of spectral features will be described using a 2 coordinate notation as $[\omega_{\text{coh}}, \omega_{\text{reph}}]$, with energies listed in wavenumbers.

In the rephasing 2DES of QDs (Fig. 1(a)), two significant features appear along the diagonal, an intense feature at $17\,500\text{ cm}^{-1}$ and a tail extending up to $19\,000\text{ cm}^{-1}$. The most intense diagonal feature is centered at $[17\,500\text{ cm}^{-1}, 17\,500\text{ cm}^{-1}]$, and shows some elongation along the diagonal, extending from $\sim 17\,000\text{ cm}^{-1}$ to $\sim 18\,250\text{ cm}^{-1}$. Strong, clearly resolved cross peaks appear both above and below the diagonal, with the lower cross peak centered at $[18\,800\text{ cm}^{-1}, 17\,500\text{ cm}^{-1}]$ and the upper cross peak centered at $[17\,350\text{ cm}^{-1}, 18\,850\text{ cm}^{-1}]$. Rephasing 2DES of the NRs (Fig. 1(b)) shows only a single resolved peak, located on the diagonal at $[17\,450\text{ cm}^{-1}, 17\,450\text{ cm}^{-1}]$. Clear diagonal elongation of the peak is evident. A lower cross peak appears as a shoulder on the diagonal peak, extending along $\omega_{\text{reph}} = 17\,400\text{ cm}^{-1}$ out to a $\omega_{\text{coh}} \approx 19\,250\text{ cm}^{-1}$. No signs of an upper cross peak are present. Rephasing 2DES of NPLs (Fig. 1(c)) show a single strong feature along the diagonal at $[18\,200\text{ cm}^{-1}, 18\,200\text{ cm}^{-1}]$. The peak is substantially less broad than either the QD or NR spectra, and shows no evidence of elongation along the diagonal. A lower cross peak appears as a low intensity shoulder extending out to $\omega_{\text{coh}} \approx 19\,000\text{ cm}^{-1}$ at $\omega_{\text{reph}} = 18\,200\text{ cm}^{-1}$, and there is no evidence of an upper cross peak.

Time evolution of 2DES

Figures 2–4 demonstrate typical time evolution of the rephasing 2DES of QDs, NRs, and NPLs, respectively. Struc-

ture apparent in the spectrum other than the four major features presented in Fig. 1 and described above, such as the low intensity cross peaks below the diagonal in the $T = 0$ QD spectrum at $\sim [18\,900\text{ cm}^{-1}, 16\,800\text{ cm}^{-1}]$, are the result of artifacts from Fourier windowing, scatter subtraction, or, at early waiting times, contributions from solvent response. These artifacts appear mostly near $T = 0$ and are less prevalent at lower pulse powers. These artifacts are easily distinguished from real signals because the artifacts are not repeatable, and they will not be discussed further. The apparent differences in appearance of $T \leq 100\text{ fs}$ 2DES and $T \geq 1\text{ ps}$ 2DES of the same material are due to slight changes in the output spectrum of the laser source for different experiments performed on different days. This is an unavoidable consequence of operating the NOPA at the bluest edge of its output range, making its output spectrum difficult to reproduce exactly in successive alignments. Different laser pulses used on different days allow more or less signal to be collected on the blue and red edges of the bandwidth. For measurements taken on the same day, with the same laser source output spectrum, all 2DES measured at $T \geq 40\text{ fs}$ look identical by visual inspection. Quantitative measures of dynamics discussed below yield the same results in all experiments, regardless of the output spectrum of the laser source. The clearest example of this effect is seen in Fig. 3, where the lower cross peak is much more well resolved in the longer waiting time spectra. The laser source provided substantially more intensity on the blue edge of the bandwidth for the later waiting time experiments, resulting in a clearer picture of the lower cross peak.

In the rephasing 2DES of QDs shown in Fig. 2, the most intense feature is slightly above the diagonal at $T = 0\text{ fs}$, shifting downwards by $\sim 150\text{ cm}^{-1}$ onto the diagonal by $T = 20\text{ fs}$ and remaining there at longer waiting times. The lower cross peak shifts downwards by about 200 cm^{-1} and increases in intensity both in an absolute sense and relative to the lower energy diagonal peak as waiting time increases from 0 to 40 fs. The rapidly decreasing intensity of the intense diagonal peak allows the higher energy diagonal feature to be seen more clearly as waiting time increases. After $T \approx 40\text{ fs}$ there is no clear evolution of the 2DES with increasing waiting time, aside from slow decay of the intensity of all features, and measurable signal levels persist out to the maximum achievable optical delays (1.2 ns). The most intense feature is typically elongated along the diagonal at all waiting times, but it is difficult to see the elongation by eye in the 2DES at longer waiting times. Figure 3 shows the time evolution of rephasing 2DES of NRs. At $T = 0\text{ fs}$, signal intensity is concentrated along the diagonal. As waiting time increases, the lower cross peak/shoulder grows in. Beyond $T \approx 40\text{ fs}$ there is no significant evolution of the spectrum with time. Figure 4 shows the time evolution of the rephasing 2DES of NPLs, showing similar dynamics to the 2DES of NRs displayed in Fig. 3. At $T = 0\text{ fs}$ there is a lone strong diagonal peak. As waiting time increases the lower cross peak grows in, reaching full strength by $\sim 40\text{ fs}$. Beyond $T \approx 40\text{ fs}$, no significant evolution of the spectrum occurs.

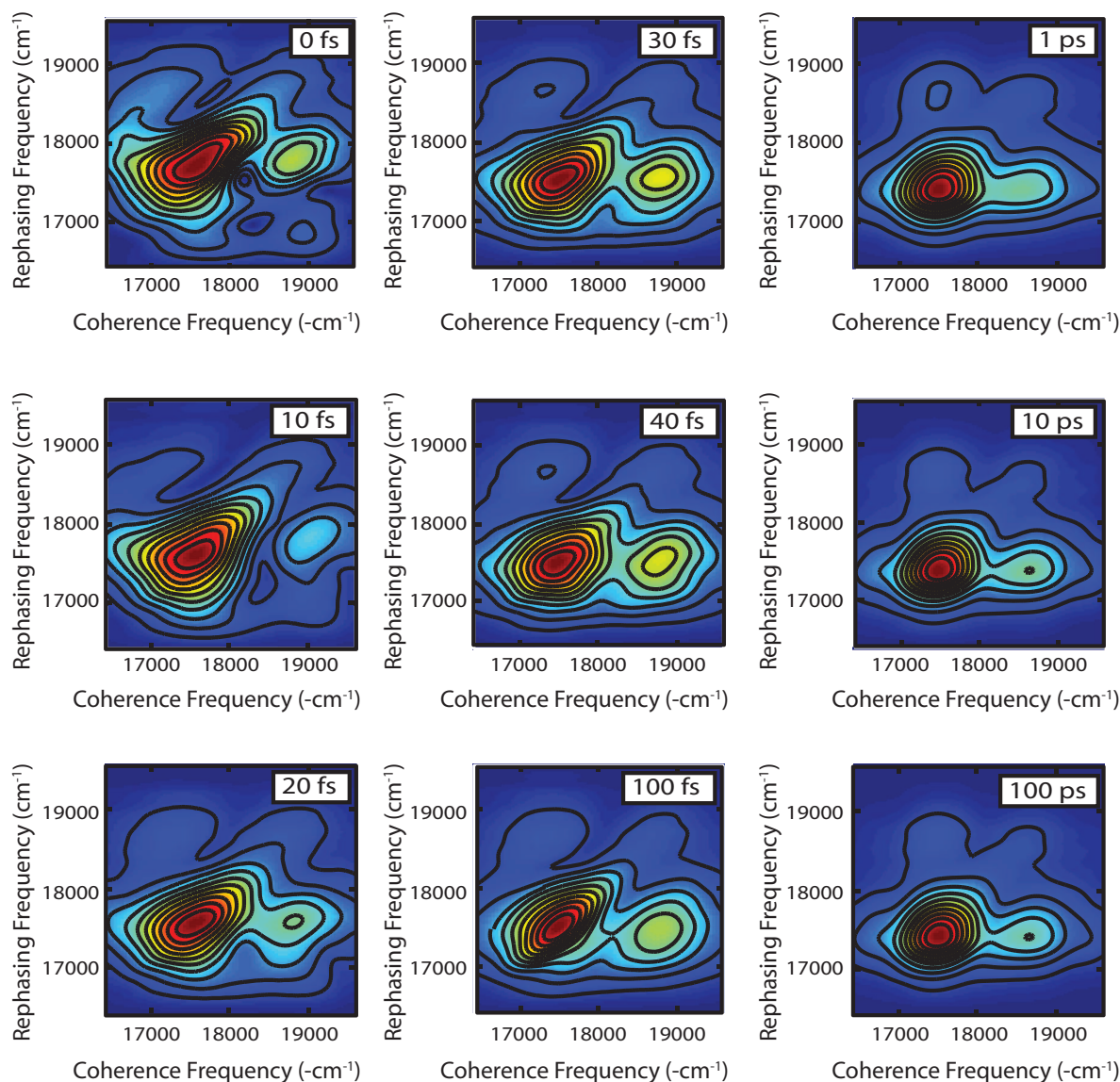


FIG. 2. Rephasing 2DES of CdSe QDs taken over a range of waiting times using a pulse power of ~ 1 nJ/pulse. The color scale in each spectrum is individually normalized to maximum intensity at that waiting time.

DISCUSSION

The QD spectra presented in Fig. 1(a) show two diagonal features, which we assign to the $1S_{3/2}-1S_e$ (lower energy, intense feature) and $2S_{3/2}-1S_e$ (higher energy shoulder) transitions in agreement with previous linear spectroscopy,²³ following the labeling scheme of Efros and Rosen.⁵ The first term (nQ_j) refers to the valence band hole state, labeled by ordinal number n , envelope angular momentum Q and total angular momentum j . The second term (nQ_e) labels the conduction band electronic state by ordinal number and envelope angular momentum. These spectra show small differences when compared to the recently published 2DES of CdSe QDs by Turner and Scholes.³¹ The four main peaks are observed in both spectra, but Turner and Scholes report additional peaks at both higher and lower rephasing energies. These peaks are assigned to contributions from biexciton states. The experiments yielding the previously reported spectra were performed at higher pulse powers (≤ 5 nJ compared

to 0.5–2.0 nJ), which should lead to stronger biexciton features, and also used larger QDs (3.0 nm radius vs. 1.75 nm radius), yielding more closely spaced electronic states due to reduced confinement. In addition, Turner and Scholes were able to phase their 2DES using a method not practicable with our instrument, and the additional features appear most prominently in the real parts of the reported spectra. In light of these experimental differences, we find good agreement when comparing the absolute value, rephasing 2DES reported here with results from the previous experiments.

The NR 2DES displayed in Fig. 1(b) show only one intense feature corresponding to the lowest energy exciton of the system. Figure 3 shows a lower cross peak growing in over the first 40 fs of waiting time, appearing as a shoulder on the intense feature. Calculations based on semi-empirical pseudopotentials^{38,48} have shown that as the rod lengthens from the spherically symmetric quantum dot towards a quantum wire the order of several of the hole states changes due to symmetry considerations. In brief, some states are much

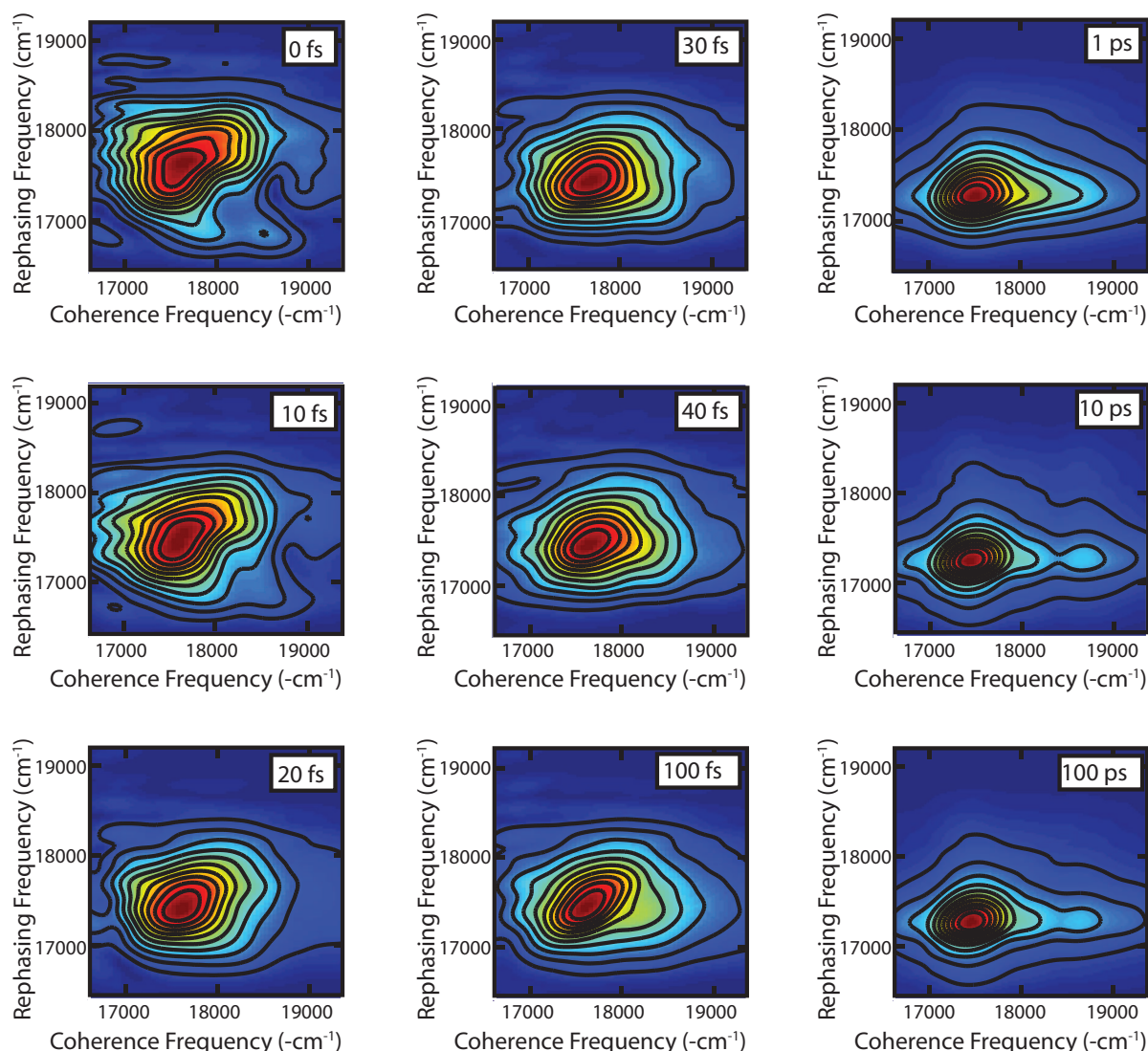


FIG. 3. Rephasing 2DES of CdSe NRs taken over a range of waiting times with a pulse power of ~ 1 nJ/pulse ($T \leq 1$ ps) or ~ 0.5 nJ/pulse ($T \geq 10$ ps). The color scale in each spectrum is individually normalized to maximum intensity at that waiting time.

more strongly dependent on confinement along the long axis of the rod than others, causing their energies to change more rapidly and eventually resulting in crossover. The NR crystals studied here have an aspect ratio of $\sim 3:1$, based on visual inspection of the TEM image presented in Fig. 1(e). In this size regime, we expect the $1S_{1/2}-1S_e$ transition to be the lowest energy transition, and we therefore assign the lone intense peak in the 2DES of the NR sample to that transition. This assignment is consistent with calculations performed specifically on large aspect ratio rods.⁶¹

The NPL 2DES, shown in Fig. 1(c), are very similar to the NR spectra, showing a lone strong feature on the diagonal. A lower cross peak is presented as a shoulder, growing in at early waiting times and remaining stationary for $T \geq 40$ fs, as shown in Fig. 4. Linear NPL spectra show two features near the bandgap usually labeled the heavy-hole and light-hole bands. Comparison of the laser output spectrum with the linear absorption spectrum of the NPL sample shows that only the heavy-hole band is firmly within the laser bandwidth. Technical complications prevent the synthesis of NPL

samples with further redshifted absorption bands, as well as the blueshifting of the laser source output. The intense feature in the NPL 2DES is assigned to the heavy-hole transition, analogous to the $1S_{1/2}-1S_e$ transition in NRs. The features in Fig. 4 are noticeably narrower than the corresponding band in the NR spectra, because confinement in the NPLs is substantially more homogenous than in NPLs or QDs. This effect has been demonstrated by linear spectroscopy of several sizes of NPLs.⁵²

Comparison of the nanocrystal spectra provides a clear demonstration of the effects of sample inhomogeneity on 2DES. Diagonal elongation of the features in the QD and NR spectra shows that the samples consist of an ensemble of nanocrystals with a range of transition frequencies caused by the finite size distributions of the nanocrystals. In contrast, the NPL spectra show rounder features and no diagonal elongation, consistent with a more homogenous ensemble. NPLs show substantially reduced inhomogeneity because confinement along the shortest dimension (the thickness of the nanoplatelet) is extremely well defined. The measured

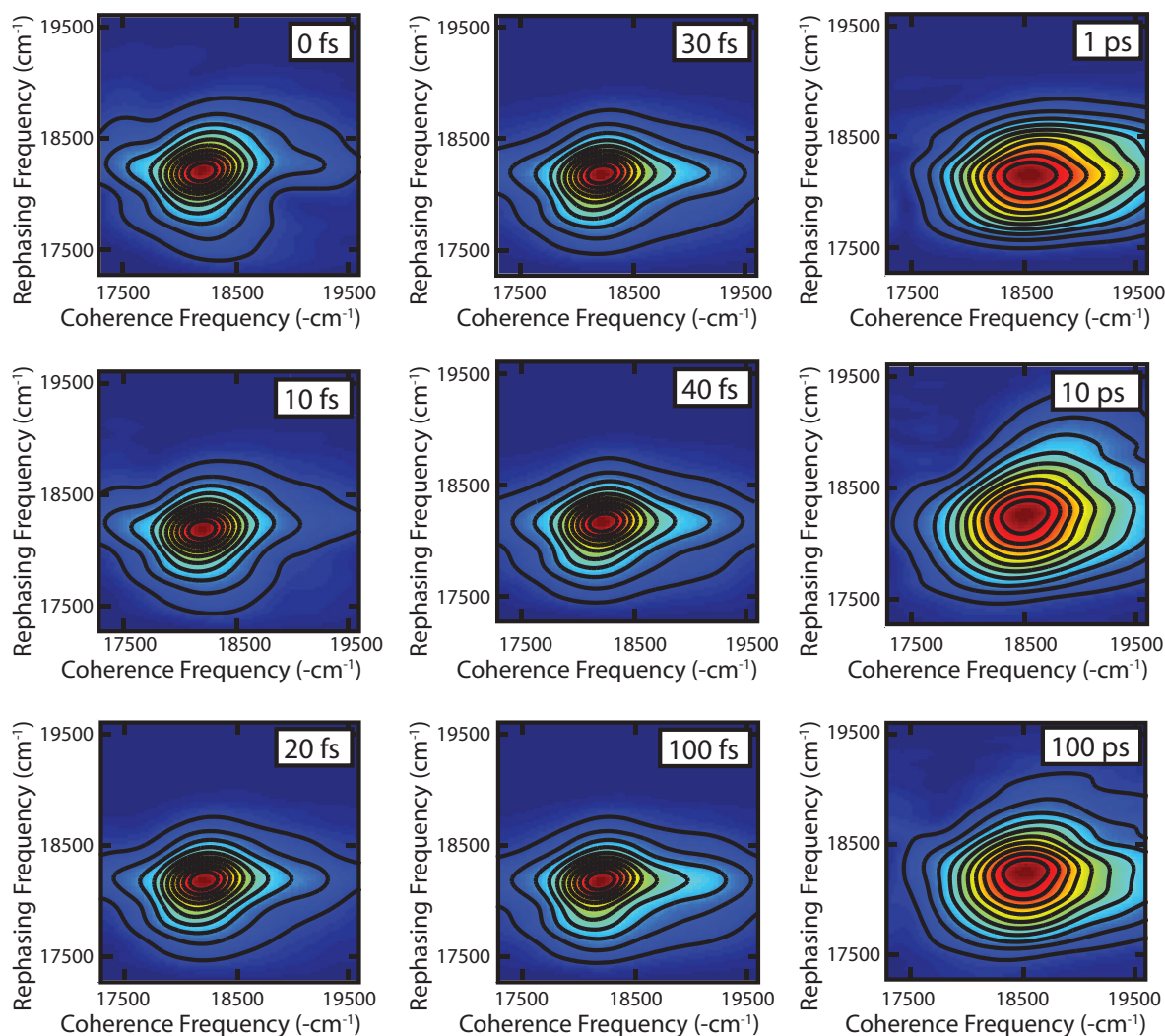


FIG. 4. Rephasing 2DES of CdSe NPLs taken over a range of waiting times with a pulse power of <1 nJ/pulse ($T \leq 1$ ps) or ~ 16 nJ/pulse ($T \geq 10$ ps). The color scale of each spectrum is normalized to the maximum intensity at that waiting time.

sample consists of NPLs made of exactly 7 CdSe monolayers. The 2DES measurements presented here do not resolve contributions from NPLs of different longitudinal dimensions, resulting in a homogenous line shape. With the ability to phase the 2DES presented here, detailed analysis of the line shapes would be possible. Because the particles do not change size, strong diagonal elongation of the cross peaks should be observed, indicating correlation of the energies of the excited states. This putative feature of 2DES has often been discussed but not, to our knowledge, yet observed experimentally.

More detailed examination of the dynamics observed in these experiments is facilitated by integrating the signal at specified spectral coordinates for each waiting time, and analysis of the QD 2DES gives the clearest interpretation because of the fully resolved and clearly assigned spectral features. Figure 5 shows the results of integrating the lower cross peak region of the 2DES at each waiting time for QDs. At early times the signal sharply increases, reaching a maximum at just over 20 fs as seen in Fig. 5(a). The signal level then decays slowly on timescales of tens to hundreds of picoseconds, as shown in Fig. 5(b). Following the “first order” interpretation of 2DES described above, we expect to observe

energy transfer from the $2S_{3/2}-1S_e$ state into the $1S_{3/2}-1S_e$ state as an exponential increase in signal at the lower cross peak spectral coordinates as waiting time increases. Figure 5 clearly demonstrates that the only time domain, within the experimentally accessible range (1.2 ns), over which the lower cross peak signal increases is the very early times shown in Fig. 5(a). All longer timescales either show no change, as in the first 1 ps shown in the left inset of Fig. 5(b), or exponential decay, as seen in the main panel of Fig. 5(b). However, we cannot assign the 20 fs increase in lower cross peak intensity to relaxation from the $2S_{3/2}$ hole state into the $1S_{3/2}$ state without accounting for two interrelated factors that complicate interpretation of 2DES at early times: pulse overlap effects and nonresonant solvent response. Pulse overlap makes it impossible to separate rephasing and nonrephasing signals at early times, because the order of interaction of the laser pulses cannot be determined when they are temporally overlapped. In Fig. 5(a), we show the expected contribution from nonresonant solvent response as a solid red line, measured in separate, solvent-only experiments and scaled for display purposes. Nonresonant solvent response contributes only positive intensity, so interference from solvent response

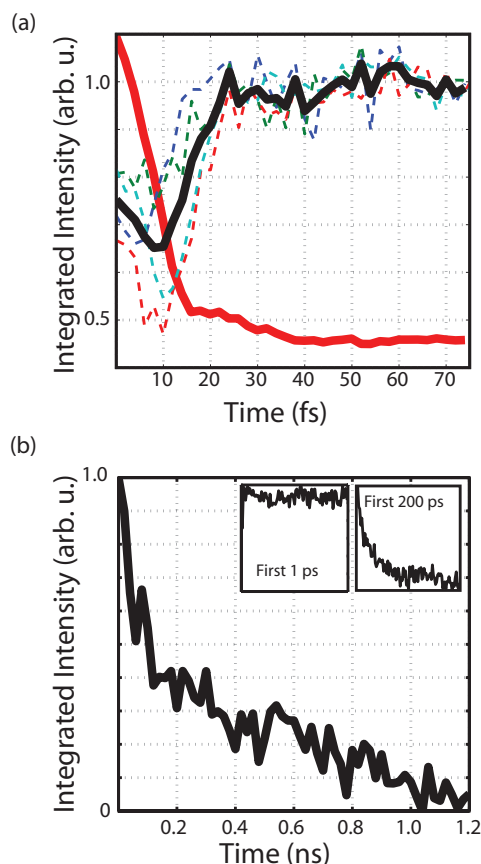


FIG. 5. Intensity of the lower cross peak in rephasing 2DES of CdSe QDs plotted against waiting time, integrated over a circular area centered at $[18\,800\text{ cm}^{-1}, 17\,500\text{ cm}^{-1}]$ with a radius of 250 cm^{-1} . (a) Early time dynamics. The black solid line shows the average intensity over four experiments run with $<1\text{ nJ/pulse}$, normalized to long time intensity, with traces for the individual experiments shown as dotted lines. The solid red line is the integrated intensity of the solvent response at the cross peak position measured in solvent-only experiments, scaled for display purposes. Nonresonant solvent response is a good measure of the pulse overlap region. Detailed comparison of the relative magnitudes of sample and solvent response is presented in detail in the supplementary material.⁵⁴ (b) Long time dynamics. The black solid line shows the full experimentally available time range, normalized to maximum intensity. Substantial intensity is still present at several hundred picoseconds. 2DES still show signal discernable above noise at 1.2 ns. The insets show shorter time ranges in more detail, demonstrating that the only time range over which the lower cross peak signal increases is over the first 40 fs, as shown in Fig. 5(a).

cannot explain the observed increase in intensity of the lower cross peak at early times, although it may distort the rising edge of the signal. Because the only increase in lower cross peak intensity is observed on a timescale similar to that of the pulse overlap, we do not attempt to fit a timescale to the rising edge of the signal, which we expect to be somewhat distorted by solvent response, but we can confidently conclude that relaxation from the $2S_{3/2}$ hole state into the $1S_{3/2}$ state occurs within the first 20 fs. This is substantially faster than previously reported electronic relaxation dynamics in CdSe QDs measured by transient absorption.^{19,21,23,46} These experiments used longer pulses, generally $\sim 100\text{ fs}$, to measure relaxation from higher lying states, but we expect that spectral overlap between the features corresponding to the 2 states discussed in this work would have made observation of these dynamics difficult in transient absorption experiments, whereas

in 2DES the feature corresponding to electronic relaxation is clearly resolved. This suggests that 2DES could be used to measure clearly resolved relaxation dynamics of the higher lying states as well, especially in larger nanocrystals with more closely spaced features. The long time relaxation dynamics shown in Fig. 5(b) are consistent with those reported by Klimov.²³

Similar relaxation dynamics were observed in both NR and NPL 2DES. In the NR spectra, a small shoulder towards higher energy, observable along the diagonal at early waiting times and shifting to lower rephasing energies as waiting time increases, as shown in Fig. 3, results from higher lying states relaxing into the $1S_{1/2}$ – $1S_e$ state. The broad, unresolved nature of the feature is likely the result of a combination of sample inhomogeneity and the reduced symmetry of the NRs relative to the QDs, which results in a much larger density of states.³⁸ The width of the shoulder in the rephasing dimension at long waiting times reflects the width of the $1S_{1/2}$ – $1S_e$ state. In the NPL spectra, a similar growing in of the lower cross peak with increasing waiting time can be seen in Fig. 4. In this case, the unresolved nature of the cross peak is solely due to an increased density of states, as sample inhomogeneity is not a factor in NPL spectra, as discussed above. In both the NR and NPL spectra, integrating the signal at the cross peak position results in dynamics identical to those presented in Fig. 5, although the choice of integration coordinates is somewhat ambiguous due to the lack of a resolved cross peak. Because the lower cross peak only appears as an unresolved shoulder in these spectra, we cannot make detailed claims about the precise nature of the relaxation. The prompt appearance of a cross peak does indicate that ultrafast relaxation from higher lying states to the lowest exciton state is occurring, but the larger density of available states prevents detailed assignment.

While recent reports of coherent superposition states in QDs³¹ are not explicitly verified by the results reported here, neither are they explicitly contradicted. These states would create an oscillating signal at the lower cross peak position, with a period of $\sim 25\text{ fs}$ corresponding to the 1300 cm^{-1} energy gap between the two states (as measured by the cross peak position $[18\,800\text{ cm}^{-1}, 17\,500\text{ cm}^{-1}]$). A slight decrease of initial intensity precedes the increase from population transfer between the states, but is likely due to interference from nonresonant solvent response. After the increase in signal intensity, i.e., beyond the pulse overlap, no reproducible oscillation in signal intensity is observed. There are several possible reasons why the two measurements of 2DES of QDs might yield different results. Spectral overlap between the laser and the absorption spectrum of the QDs used is slightly different in the two experiments, with the previous work favoring the higher lying excited state more heavily. Previous experiments were performed at higher pulse powers, which may lead to interference from multiexciton effects. The particles used were also substantially different in the two experiments. Here, we measure 2DES from wurtzite crystals with a radius of 1.75 nm , while in the previous work 3.0 nm zinc-blende crystals were used. Although particle size should have no effect on the ability of a nanoparticle to support coherent superposition states, it is possible that the more

complicated fine structure of the wurtzite crystals is blurring out the oscillating signal. Considering the extremely small spacing of the fine structure levels (total splitting ≈ 31 meV $= 180$ cm $^{-1}$) relative to the large space of the two exciton states (~ 1300 cm $^{-1}$) we find this explanation extremely unlikely. For example, a 1000 cm $^{-1}$ level spacing yields an oscillating signal with a period of 33 fs, and we would not expect the sum of oscillations with periods of 25 and 33 fs to be a stationary signal.

There are many possible future applications of nonlinear spectroscopy in the field of nanomaterials, leveraging the ability of 2DES to eliminate inhomogeneous broadening caused by the unavoidable finite size distribution of nanocrystal samples. Experiments similar to those presented here, but performed on larger crystals with more closely spaced features, should enable unambiguous measurement of hole relaxation from the higher lying $1P_{3/2}$ state into both the $2S_{3/2}$ and $1S_{3/2}$ states in QDs, and may be able to resolve higher lying features in NRs. Two-color experiments could be used to measure dynamics in higher lying excited states. Phasing the spectra and looking at only the real part of the signal would allow for enhanced resolution and observation of correlation between excited states during relaxation via diagonally elongated cross peaks, a spectral feature that has been proposed but never observed in 2DES. Most interestingly, application of single-shot 2DES techniques and modern kHz CCD detector technology^{62,63} could allow for real-time observation of the evolution of the sample size distribution during crystal growth, although the experiment would be limited by the available laser source bandwidth because nanocrystal transition energies shift substantially as size increases.

CONCLUSION

We have used two-dimensional electronic spectroscopy to investigate the effects of particle shape on spectra and relaxation dynamics in QDs, NRs, and NPLs. The spectra verify that a substantial difference exists between the electronic structure of the lowest lying exciton states (within ~ 1500 cm $^{-1}$ of the bandgap) of QDs and those of NRs and NPLs, which we attribute to reduced symmetry in the NRs and NPLs leading to an increase in the density of charge carrier states. Ultrafast dynamics measurements suggest that ultrafast hole relaxation occurs within 30 fs in all 3 types of particles. In QDs, the transition can be assigned to relaxation from the $2S_{3/2}$ – $1S_e$ exciton state into the $1S_{3/2}$ – $1S_e$ state. In NRs and NPLs, no detailed assignment can be made because the states cannot be resolved. The QD spectra show no evidence of coherent superpositions of exciton states, in contrast to previous reports on similar nanocrystals. The NPL 2DES are the first nonlinear optical measurements of those nanocrystals, and clearly show the increased sample homogeneity relative to QD and NR samples.

ACKNOWLEDGMENTS

The authors would like to thank NSF MRSEC (Grant No. DMR 08-02054), The Keck Foundation, AFOSR (Grant

No. FA9550-09-1-0117), and DTRA (HDTRA1-10-1-0091 P00002) for supporting this work.

- ¹V. Klimov, *Annu. Rev. Phys. Chem.* **58**, 635 (2007).
- ²G. Scholes, *Adv. Funct. Mater.* **18**, 1157 (2008).
- ³P. Kambhampati, *Acc. Chem. Res.* **44**, 1 (2011).
- ⁴A. Ekimov, F. Hache, M. Schanneklein, D. Ricard, C. Flytzanis, I. Kudryavtsev, T. Yazeva, A. Rodina, and A. Efros, *J. Opt. Soc. Am. B* **10**, 100 (1993).
- ⁵A. Efros and M. Rosen, *Annu. Rev. Mater. Sci.* **30**, 475 (2000).
- ⁶C. Burda, X. Chen, R. Narayanan, and M. El-Sayed, *Chem. Rev.* **105**, 1025 (2005).
- ⁷A. Ekimov and A. Onushchenko, *JETP Lett.* **34**, 345 (1981).
- ⁸A. Henglein, *Ber. Bunsenges. Phys. Chem.* **86**, 301 (1982).
- ⁹C. Leatherdale, W. Woo, F. Mikulec, and M. Bawendi, *J. Phys. Chem. B* **106**, 7619 (2002).
- ¹⁰C. Murray, D. Norris, and M. Bawendi, *J. Am. Chem. Soc.* **115**, 8706 (1993).
- ¹¹M. Mohamed, C. Burda, and M. El-Sayed, *Nano Lett.* **1**, 589 (2001).
- ¹²D. Norris and M. Bawendi, *Phys. Rev. B: Condens. Matter* **53**, 16338 (1996).
- ¹³V. Soloviev, A. Eichhofer, D. Fenske, and U. Banin, *J. Am. Chem. Soc.* **122**, 2673 (2000).
- ¹⁴V. Soloviev, A. Eichhofer, D. Fenske, and U. Banin, *Phys. Status Solidi B* **224**, 285 (2001).
- ¹⁵N. Soloviev, A. Eichhofer, D. Fenske, and U. Banin, *J. Am. Chem. Soc.* **123**, 2354 (2001).
- ¹⁶M. Nirmal, C. Murray, and M. Bawendi, *Phys. Rev. B: Condens. Matter* **50**, 2293 (1994).
- ¹⁷D. Norris, A. Sacra, C. Murray, and M. Bawendi, *Phys. Rev. Lett.* **72**, 2612 (1994).
- ¹⁸S. Sewall, R. Cooney, and P. Kambhampati, *Appl. Phys. Lett.* **94**, 243116 (2009).
- ¹⁹P. Guyot-Sionnest, M. Shim, C. Matrangola, and M. Hines, *Phys. Rev. B: Condens. Matter* **60**, R2181 (1999).
- ²⁰C. Burda, S. Link, M. Mohamed, and M. El-Sayed, *J. Phys. Chem. B* **105**, 12286 (2001).
- ²¹E. McArthur, A. Morris-Cohen, K. Knowles, and E. Weiss, *J. Phys. Chem. B* **114**, 14514 (2010).
- ²²D. Norris and M. Bawendi, *J. Chem. Phys.* **103**, 5260 (1995).
- ²³V. Klimov, *J. Phys. Chem. B* **104**, 6112 (2000).
- ²⁴M. Lupo, F. Della Sala, L. Carbone, M. Zavelani-Rossi, A. Fiore, L. Luer, D. Polli, R. Cingolani, L. Manna, and G. Lanzani, *Nano Lett.* **8**, 4582 (2008).
- ²⁵P. Yu, J. Nedeljkovic, P. Ahrenkiel, R. Ellingson, and A. Nozik, *Nano Lett.* **4**, 1089 (2004).
- ²⁶J. He, H. Zhong, and G. Scholes, *Phys. Rev. Lett.* **105**, 046601 (2010).
- ²⁷G. Scholes, J. Kim, C. Wong, V. Huxter, P. Nair, K. Fritz, and S. Kumar, *Nano Lett.* **6**, 1765 (2006).
- ²⁸M. Graham, Y. Ma, and G. Fleming, *Nano Lett.* **8**, 3936 (2008).
- ²⁹M. Salvador, P. Nair, M. Cho, and G. Scholes, *Chem. Phys.* **350**, 56 (2008).
- ³⁰C. Wong and G. Scholes, *J. Phys. Chem. A* **115**, 3797 (2011).
- ³¹D. Turner, Y. Hassan, and G. Scholes, *Nano Lett.* **12**, 880 (2012).
- ³²L. Brus, *J. Chem. Phys.* **79**, 5566 (1983).
- ³³V. Huxter, V. Kovalevskij, and G. Scholes, *J. Phys. Chem. B* **109**, 20060 (2005).
- ³⁴V. Huxter and G. Scholes, *J. Chem. Phys.* **125**, 144716 (2006).
- ³⁵M. Salvador, M. Graham, and G. Scholes, *J. Chem. Phys.* **125**, 184709 (2006).
- ³⁶A. Franceschetti and A. Zunger, *Phys. Rev. Lett.* **78**, 915 (1997).
- ³⁷S. Sewall, A. Franceschetti, R. Cooney, A. Zunger, and P. Kambhampati, *Phys. Rev. B: Condens. Matter* **80**, 081310 (2009).
- ³⁸J. Hu, L. Wang, L. Li, W. Yang, and A. Alivisatos, *J. Phys. Chem. B* **106**, 2447 (2002).
- ³⁹J. Li and L. Wang, *Nano Lett.* **3**, 1357 (2003).
- ⁴⁰Q. Zhao, P. Graf, W. Jones, A. Franceschetti, J. Li, L. Wang, and K. Kim, *Nano Lett.* **7**, 3274 (2007).
- ⁴¹O. Prezhdo, *Acc. Chem. Res.* **42**, 2005 (2009).
- ⁴²K. Hyeon-Deuk and O. Prezhdo, *ACS Nano* **6**, 1239 (2012).
- ⁴³T. Sadowski and R. Ramprasad, *Phys. Rev. B: Condens. Matter* **76**, 235310 (2007).
- ⁴⁴V. Klimov, A. Mikhailovsky, D. McBranch, C. Leatherdale, and M. Bawendi, *Science* **287**, 1011 (2000).

- ⁴⁵M. Achermann, A. Bartko, J. Hollingsworth, and V. Klimov, *Nat. Phys.* **2**, 557 (2006).
- ⁴⁶K. Knowles, E. McArthur, and E. Weiss, *ACS Nano* **5**, 2026 (2011).
- ⁴⁷V. Klimov, A. Mikhailovsky, D. McBranch, C. Leatherdale, and M. Bawendi, *Phys. Rev. B: Condens. Matter* **61**, 13349 (2000).
- ⁴⁸L. Li, J. Hu, W. Yang, and A. Alivisatos, *Nano Lett.* **1**, 349 (2001).
- ⁴⁹L. Chen, H. Bao, T. Tan, O. Prezhdo, and X. Ruan, *J. Phys. Chem. C* **115**, 11400 (2011).
- ⁵⁰G. Cantele, D. Ninno, and G. Iadonisi, *Nano Lett.* **1**, 121 (2001).
- ⁵¹S. Ithurria and B. Dubertret, *J. Am. Chem. Soc.* **130**, 16504 (2008).
- ⁵²S. Ithurria, M. Tessier, B. Mahler, R. Lobo, B. Dubertret, and A. Efros, *Nature Mater.* **10**, 936 (2011).
- ⁵³S. Ithurria, G. Bousquet, and B. Dubertret, *J. Am. Chem. Soc.* **133**, 3070 (2011).
- ⁵⁴See supplementary material at <http://dx.doi.org/10.1063/1.4772465> (i) for verification of the crystal structures of each type of nanocrystal by X-ray diffraction; (ii) for comparison of typical linear absorption spectra of each type of nanocrystal with laser spectra; (iii) for details of the TG-FROG procedure and results; (iv) for a description of data processing procedures; (v) for discussion of the role of solvent response in high pulse power experiments; (vi) for comparison of combined, rephasing, and nonrephasing two-dimensional spectra; (vii) for a brief description of detailed interpretation of 2DES via Feynmann pathways; and (viii) for comparison of the magnitudes of resonant signal and nonresonant solvent response.
- ⁵⁵L. Carbone, C. Nobile, M. De Giorgi, F. Sala, G. Morello, P. Pompa, M. Hytch, E. Snoeck, A. Fiore, I. Franchini, M. Nadasan, A. Silvestre, L. Chiodo, S. Kudera, R. Cingolani, R. Krahne, and L. Manna, *Nano Lett.* **7**, 2942 (2007).
- ⁵⁶Z. Peng and X. Peng, *J. Am. Chem. Soc.* **124**, 3343 (2002).
- ⁵⁷T. Brixner, T. Mancal, I. Stiopkin, and G. Fleming, *J. Chem. Phys.* **121**, 4221 (2004).
- ⁵⁸J. Hybl, A. Ferro, and D. Jonas, *J. Chem. Phys.* **115**, 6606 (2001).
- ⁵⁹M. Cowan, J. Ogilvie, and R. Miller, *Chem. Phys. Lett.* **386**, 184 (2004).
- ⁶⁰V. Klimov, D. McBranch, C. Leatherdale, and M. Bawendi, *Phys. Rev. B: Condens. Matter* **60**, 13740 (1999).
- ⁶¹A. Shabaev and A. Efros, *Nano Lett.* **4**, 1821 (2004).
- ⁶²E. Harel, A. Fidler, and G. Engel, *Proc. Natl. Acad. Sci. U.S.A.* **107**, 16444 (2010).
- ⁶³E. Harel, A. Fidler, and G. Engel, *J. Phys. Chem. A* **115**, 3787 (2011).